SERI/TP-211-1984
UC Category: 60
DE83011960

The SERI Advanced and Innovative Wind Energy Concepts Program

Richard L. Mitchell
Eric W. Jacobs

June 1983

Presented at the 1983 Annual Meeting of the
American Solar Energy Society
Minneapolis, Minnesota
1-3 June 1983

Prepared under Task No. 1067.10
WPA No. 171

Solar Energy Research Institute
A Division of Midwest Research Institute

1617 Cole Boulevard
Golden, Colorado 80401

Prepared for the
U.S. Department of Energy
Contract No. EG-77-C-01-4042

Printed in the United States of America
Available from:
National Technical Information Service
U.S. Department of Commerce
5285 Port Royal Road
Springfield, VA 22161
Price:
Microfiche $4.50
Printed Copy $ 7.00

THE SERI ADVANCED AND INNOVATIVE WIND ENERGY CONCEPTS PROGRAM

Richard L. Mitchell
Eric W. Jacobs
Solar Energy Research Institute
1617 Cole Boulevard
Golden, CO 80401

ABSTRACT

In 1978 the Solar Energy Research Institute (SERI) was given the responsibility of managing the Advanced and Innovative Wind Energy Concepts (AIWEC) Task by the U.S. Department of Energy (DOE). The objective of this program has been to determine the technical and economic potential of advanced wind energy concepts. Assessment and R&D efforts in the AIWEC program have included theoretical performance analyses, wind tunnel testing, and/or costing studies. Concepts demonstrating sufficient potential undergo prototype testing in a Proof-of-Concept research phase. Several concepts, such as the Dynamic Inducer, the Diffuser Augmented Wind Turbine, the Electrofluid Dynamic Wind-Driven Generator, the Passive Cyclic Pitch concept, and higher performance airfoil configurations for vertical axis wind turbines, have recently made significant progress. The latter has currently reached the Proof-of-Concept phase. The present paper provides an overview of the technical progress and current status of these concepts.

1. INTRODUCTION

The Advanced and Innovative Wind Energy Concepts (AIWEC) program at the Solar Energy Research Institute (SERI) has been responsible for supporting the research and development (R&D) of innovative wind energy concepts since FY 1978. The origins of the AIWEC program can be traced through the Department of Energy (DOE) and the Energy Research and Development Administration (ERDA) to the National Science Foundation (NSF). The program objective has been to determine the potential of AIWEC for technically and economically viable wind energy conversion.

Other than necessary in-house technical support, the research conducted under the AIWEC program has been performed on a subcontract basis by private companies and universities. These R&D efforts have incorporated preliminary technical and cost assessments, theoretical analyses, experimental studies, conceptual designs, and detailed cost studies of AIWEC. The concepts investigated by the program have included higher performance airfoils for Darrieus-type vertical axis wind turbines (VAWT), diffuser augmentation, vortex augmentation, electrofluid dynamics, Magnus rotor systems, energy from humid air, dynamic inducers, oscillating vanes, passive cyclic pitch variation with automatic furl or yaw control, and tethered high altitude wind energy systems.

The final phase of R&D in the AIWEC program is the Proof-of-Concept testing of a prototype to verify the technical feasibility of a promising concept. A number of AIWEC have shown some technical and economic potential and the Passive Cyclic Pitch concept has reached the Proof-of-Concept phase. The status of R&D on the Passive Cyclic Pitch concept and four other promising AIWEC, (i.e., the Diffuser Augmented Wind Turbine (DAWT) the Electrofluid Dynamic (EFD) wind-driven generator, and the Dynamic Inducer (DI), and higher performance airfoil configurations for VAWT) is the topic of the present paper. Each of these concepts has, to a varying degree, shown some potential for cost-competitive wind energy conversion. An assessment of another technically promising concept, tethered wind energy systems, can be found in Reference 1.

2. THE ELECTROFLUID DYNAMIC (EFD) WIND-DRIVEN GENERATOR

The basic principle behind the EFD concept is the use of an aerosol particle as the active element in a drag type Wind Energy Conversion System (WECS). These particles—liquid droplets or hollow spheres (bubbles)—are charged and carried by the wind into an electrical field. This field exerts an electrical force on the particles that is opposite to the wind direction. In overcoming the electrical force, the particles extract the kinetic energy from the wind through the drag force exerted on them. Unlike a conventional WECS that uses a mechanical coupling between the active elements and the generator, the EFD generator uses an electrical field coupling. An advantage of this arrangement is that it requires a minimum of moving components.

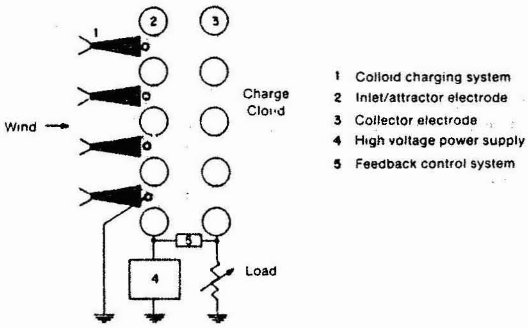

Fig. 1. Schematic of the EFD Wind-Driven Generator (from Ref. 3).

This system has two main parts: the colloid charging section and the working section. As shown in Figure 1, the working section consists of an inlet/attractor electrode (item 2) and a collector electrode (item 3). The aerosol is charged with one polarity by a corona discharge wire or other charging system (item 1) and enters the working area. The wind then pushes the charged particle up the potential hill to the collector electrode. At this point the charged cloud, formed behind the EFD rig following start-up, aids the collector electrode in the collection of the charged particles. The high voltage power supply and feedback control system (items 4 and 5) ensure that the charge is drained at an adequate rate and that the field voltage is optimum for the working section. The concept typically uses very high voltage and low current (330 kV, 15 $\mu A/m^2$).

Research on the EFD wind-driven generator has been underway at the University of Dayton since 1975 (2,3,4,5). Support for this research has been provided by the NSF, ERDA, DOE, and SERI. These efforts have resulted in the development of analytical models for aerosol and generator performance, thereby providing a detailed analytical model of the EFD system including field mapping, field breakdown limits, geometric parameters, and performance characteristics. Wind tunnel configurations have been tested to verify the theoretical models (Figures 2 and 3).

The wind tunnel tests have indicated that the more important parameters are particle mobility, electrode diameter, vertical electrode spacing, horizontal electrode spacing, field voltage, and wind velocity. Early efforts demonstrated that water droplets, although good performers in an EFD concept, could not be generated with the low mobilities required for high efficiency operation. Therefore, subsequent research efforts were concentrated on the production of low mobility bubbles, which can be generated either singly or in agglomerates with the necessary mobility. Analysis of the optimum configuration for a full-size bubble generator, including pumping and charging requirements, produced encouraging results as shown in Figure 4.

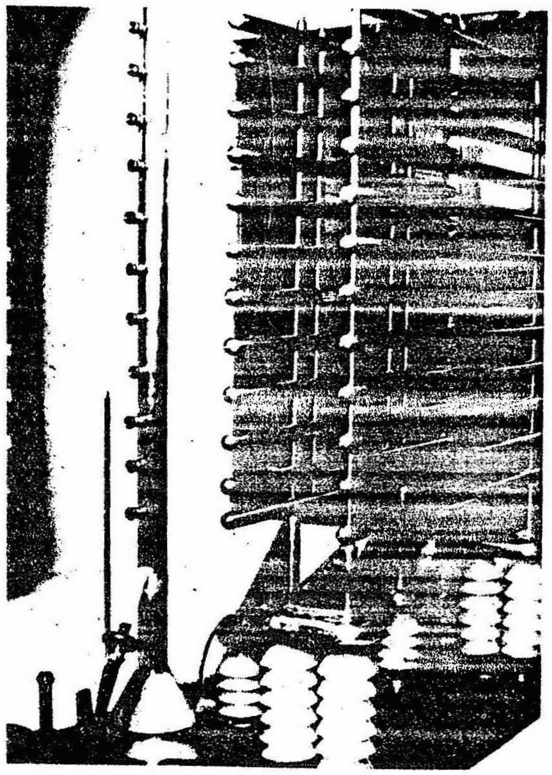

Fig. 2. EFD Wind Tunnel Test Rig.

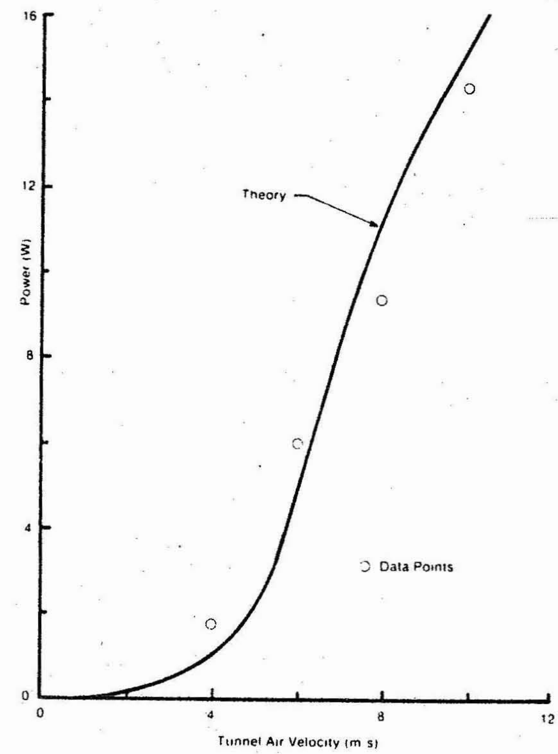

Fig. 3. Comparison of EFD Wind Tunnel Data with Theory.

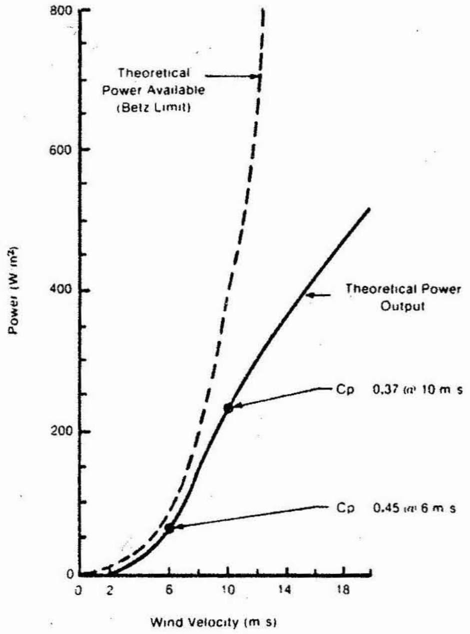

Fig. 4. Theoretical EFD Power Output Density vs. Wind Speed.

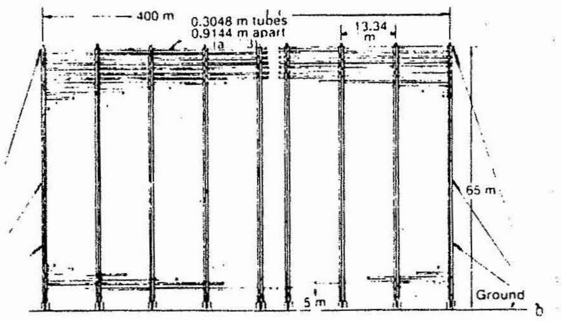

Fig. 5. Frontal View of the EFD Conceptual Design (from Ref. 6).

2.1 Conceptual Design of an EFD Wind-Driven Generator

Based on the promising studies conducted to date, the current SERI-supported effort is pursuing the development of a conceptual design for an EFD wind generator (6). The University of Dayton has established the design parameters, with particular attention to the material requirements versus system performance. The conceptual design (Figure 5) has a working section 5m (16.4 ft) to 65m (213.2 ft) in height with a width of 400m (1312 ft) giving a wind energy conversion area of 24,000m^2 (258,200 ft^2). The SERI estimate (7) of annual energy output (AEO) is 62 W/m^2 or 13,000 MWh based on an average annual wind speed of 6 m/s (13.4 mph), a 1/7 power law height variation of wind speed, and a wind rose with a highly predominant wind direction such as that of Honolulu (8). The latter assumption is necessary as the conceptual design lacks any yaw capability. When corrected for height differences, this AEO estimate is 46% of the MOD-2 prediction for a 6.3 m/s (14 mph) wind site (9). Thus the AEO estimate for the EFD conceptual design appears to be suitably conservative.

Cost estimates of this EFD conceptual design were developed at SERI, using a detailed estimate of material and labor requirements from "Richardson Process Plant Construction Estimating Standards" and information from manufacturers of specialized equipment. The estimated cost of a single unit constructed on site, including all overhead and profit but without making provisions for land cost and without incorporating manufacturing or learning curves, is $23,073,000. Using the DOE Cost of Energy equation, the annualized cost of energy (COE) of the EFD system is:

$$\text{COE} = \frac{\$23{,}073{,}000 \times 0.18}{13{,}000{,}000 \text{ kWh}} = 31.9 \text{ cents/kWh.} \tag{1}$$

O&M costs, assumed to be small relative to conventional wind energy systems, have not been included in this calculation.

The estimated 100th unit cost is $15,724,000, for an annualized COE of 21.8 cents/kWh. Additional cost reductions could be obtained by further

Wind System	Mass (Mg)	Energy/Mass (kWh/kg)	Mass/ Conversion Area (kg/m^2)	Energy/ Conversion Area kWh/m^2
Sandia Darrieus (1)	3.82	15.7	45.7	717.5
Giromill	9.07	20.9	40.1	838.1
Sandia Darrieus (2)	11.51	19.9	41.3	821.9
Magdalen Island Darrieus	22.00	17.6	37.0	651.2
Hutter	13.15	27.8	14.4	400.3
MOD-OA	40.37	22.1	35.4	782.3
MOD-X	33.08	28.7	29.0	832.3
EFD	1,721.50	7.5	71.7	539.9
MOD-1	297.00	15.0	102.0	1530.0

Table 1. Mass and Wind Energy Value Indicators

optimization of the conceptual design. However, the preliminary nature of the design studies are not detailed enough to establish a definitive range for a cost reduction. Projected reductions range from very modest to well below the previous prediction.

Due to the variances in costing estimates, it is useful to look at other parameters such as the mass and wind energy value indicators shown in Table 1 (10,11). As shown, the EFD concept is within the range of most wind systems with respect to kWh/m^2 but is extremely material intensive. This material intensity could be compensated for if the kWh/m^2 value were not at the lower end of the range. The material intensity will have a negative impact on the system potential if it cannot be improved upon. However, significant optimization potential exists for the EFD concept and the value indicators could range from very marginal to acceptable compared to conventional wind energy systems. Further research is needed to establish more accurate estimates of EFD annual energy output and value indicators with narrower ranges.

3. THE DIFFUSER AUGMENTED WIND TURBINE (DAWT)

The DAWT concept, shown in Figure 6, employs a conventional horizontal axis wind turbine (HAWT) with an added diffuser shroud to provide flow, and hence power, augmentation. The diffusion or expansion of the flow within the shroud causes a static pressure increase, thus permitting a lower static pressure just downstream of the turbine and a correspondingly greater pressure drop across the rotor disk. The increased pressure drop induces a greater mass flow of air through the turbine as shown in Figure 7.

Research on the DAWT has been conducted by Grumman Aerospace Corporation since 1973 and has been supported by ERDA, DOE, and SERI since 1976. Previous R&D on diffuser shrouds (13) had demonstrated the augmentation effect. However, these research efforts concentrated on costly, long, narrow angle (half angles $<6°$)

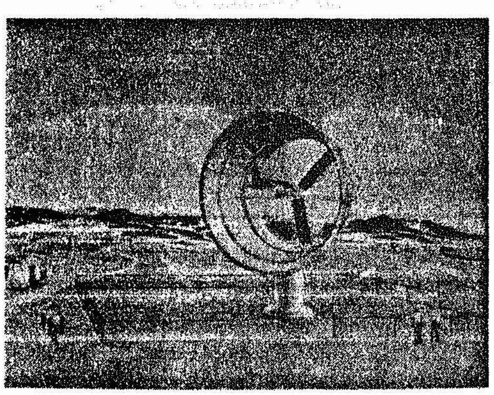

Fig. 6. Sketch of a DAWT (from Ref. 12).

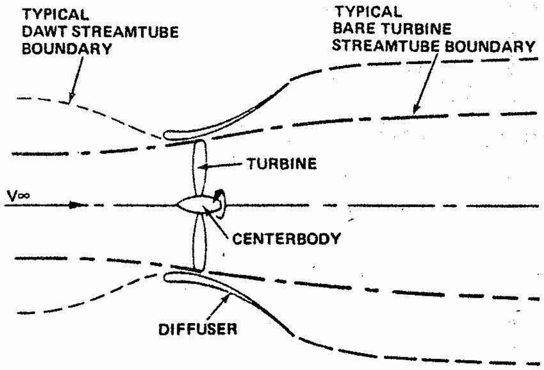

Fig. 7. Schematic of DAWT Flow Field Compared to that of a Bare Turbine (from Ref. 12).

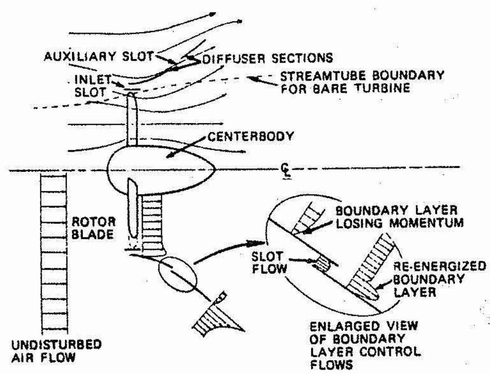

Fig. 8. Schematic of DAWT Flow Field Showing Boundary Layer Regeneration (from Ref. 14).

diffusers to prevent boundary layer separation. A major objective of the Grumman research has been to develop less costly short, wide angle diffusers. Half-angles of 30 to 45° have been achieved with the use of slots in the diffuser wall to provide boundary layer regeneration and thus prevent flow separation (Figure 8).

Initial DAWT research by Grumman involved open jet wind tunnel testing of small models (0.045m inlet diameter) (15). Subsequent research with a larger model (14) used the design parameters established in the small model tests. The larger model had a rotor diameter of 0.46m (1.5 ft), a diffuser exist to rotor area ratio of 2.78 and a half-angle of 30°. Testing of this model in a 2.1m x 3m (7 ft x 10 ft) wind tunnel provided peak power coefficient (c_p) augmentation ratios of ~3.0 based on the Betz limit and ~4.1 based on bare turbine performance.

Further efforts were supported by SERI to establish the engineering and cost parameters for a full-size DAWT system based on the wind tunnel data for the larger model. The results of this study (16) indicated that the DAWT concept has a potential for cost-competitive wind energy conversion. Estimated costs of energy (COE)

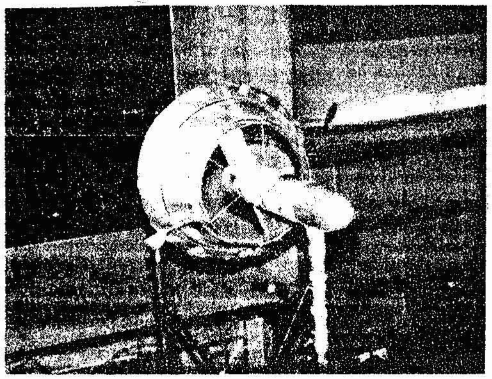

Fig. 9. 30° DAWT Model in the 1.8m x 1.8m Open Jet Wind Tunnel.

were 7.5 to 12 cents/kWh for small DAWT (~11 kw) and 4 to 6 cents/kWh for large DAWT (~150 kW). These COE were obtained by using Equation (1). Note, however, that the annual energy output (AEO) estimates used in the study require further verification.

Current research has been directed towards optimizing DAWT design parameters to increase performance and decrease cost. The larger DAWT model has been retested (17) in a 1.8m x 1.8m (6 ft x 6 ft) open jet wind tunnel with an improved rotor design (Figure 9). In addition, a shorter, more compact diffuser model with a half-angle of 45° was also tested. The 45° model employed radial flanges at the diffuser exit which provided exit-to-rotor area ratios of 2.55 to 3.17 without changes in diffuser length. This latter configuration is designated the dump diffuser.

The open jet wind tunnel tests of the 30° model resulted in augmentation ratios of ~3.0 based on the Betz limit and ~5.0 compared to the bare rotor performance. The corresponding results for the 45° dump diffuser were ~3.3 and ~5.6 respectively. These results, along with those from the Grumman wind tunnel, are summarized in Table 2. The Grumman wind tunnel result based on the Betz limit may be high due to systematic test errors, thus indicating that the corresponding augmentation ratio based on bare rotor performance is more reliable. The 45°

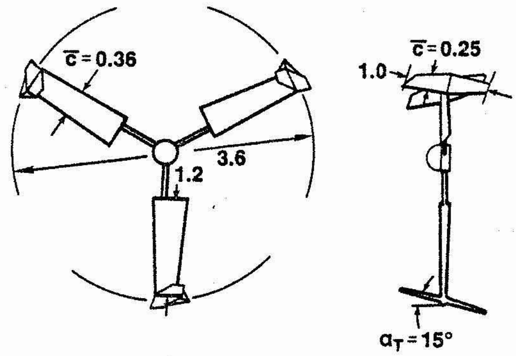

Fig. 10. Views of Prototype Scale Dynamic Induces (dimensions in meters) (from Ref. 19).

results were obtained with an area ratio of 2.62 corresponding to a flange width of 1.5% of the diffuser exit diameter. Using the exit area rather than the rotor area gives a power augmentation of ~1.25 based on the Betz limit for the 45° model. Another important result of the open jet wind tunnel test was the demonstration of nearly constant power augmentation over a broad range of tip speed ratio. Thus the increase in AEO could be nearly equivalent to the augmentation ratio at peak power coefficient.

4. THE DYNAMIC INDUCER

The operating principle of the Dynamic Inducer, shown in Figure 10, is similar to that of the DAWT concept. Unlike the passive shroud of the DAWT, however, the augmentation elements of the Dynamic Inducer are active, consisting of tip vanes mounted at approximately right angles to the blade tips of a conventional HAWT. When the turbine is rotating, these tip vanes create a lifting force acting in a radially outward direction, thereby causing an expansion of the streamtube. As with the DAWT, this expansion results in a lowered subatmospheric static pressure behind the rotor disk, an increased pressure drop across the turbine, and thus an increased mass flow rate through the turbine.

Model/Test	Based on Betz Limit ($C_{p,Betz}$=0.593)	Based on Bare Rotor Performance
30° - Grumman Wind Tunnel	3.4	4.1
30° - VPI Wind Tunnel	3.0	5.0
45° - VPI Wind Tunnel	3.3	5.6

Table 2. Experimentally Observed Augmentation Ratios of Peak Power Coefficient by the DAWT.

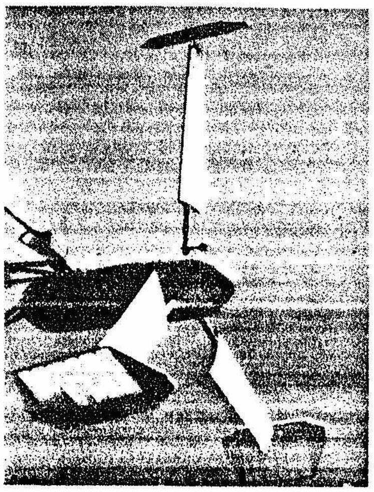

Fig. 11. Tow Test Model of the Dynamic Inducer.

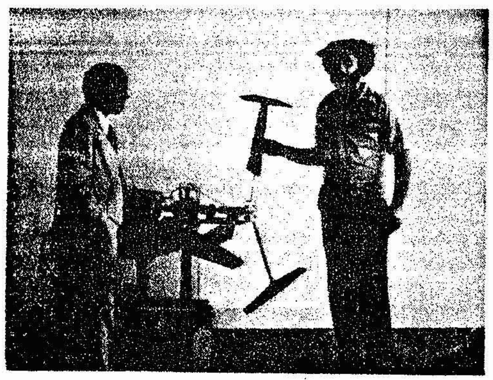

Fig. 12. Wind Tunnel Model of the Dynamic Inducer.

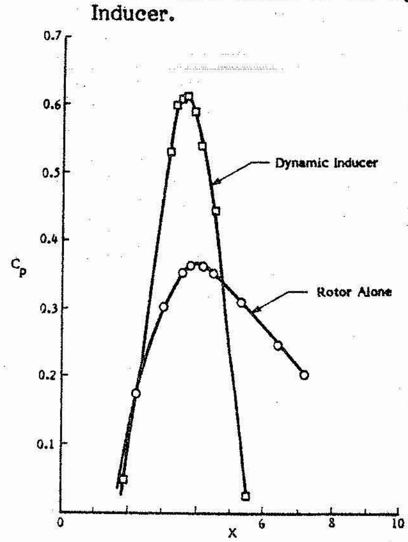

Fig. 13. Power Coefficient (c_p) vs. Tip Speed Ratio (X) for the Dynamic Inducer and the Bare Rotor (from Ref. 19).

Research on the Dynamic Inducer has been conducted by AeroVironment, Inc., with the support of ERDA, DOE and SERI since 1977. The initial efforts included tow testing of a 3.6m (12 ft) diameter rotor, shown in Figure 11, in which no augmentation effect was observed (18). The lack of augmentation was traced to parasitic drag losses associated with the tip vane blade connections and subsequent efforts were concentrated on the solution of this problem. An improved analytical model was developed and applied to the design and construction of a 1.2m (4 ft) diameter, three-bladed model of the Dynamic Inducer. Wind tunnel tests of this model (Figure 12) showed, based on bare rotor disk area, an increase in peak power coefficient (c_p) of ~70% over the bare rotor measurement when corrected for wind tunnel blockage effects (19). However, as shown in Figure 13, the power coefficient versus tip speed ratio (X) curve was much narrower and more sharply peaked for the Dynamic Inducer. A narrow, sharply peaked tip speed ratio curve would have significantly adverse effects on Dynamic Inducer COE. Further tow testing of the 3.6m (12 ft) diameter model with improved tip vane blade connections yielded a lower increase of ~35% for the peak power coefficient, again based on bare rotor disk area.

Current research efforts have been directed toward tip vane and rotor optimization (19). Tests have been conducted in a 2.4m x 3m (8 ft x 10 ft) water channel with a 0.51m (1.67 ft) diameter, two-bladed low solidity rotor and several tip vane configurations. Wake surveys showed that the tip vanes were providing significant flow augmentation. However, low shaft power levels relative to theoretical predictions were observed due to high drag losses. Comparisons of theoretical and observed performance based on shaft power and wake deficit measurements for two test runs in the water channel are shown in Table 3. The results given for run no. 48 in Table 3 demonstrate that, although a greater flow augmentation effect was found at the higher tip speed ratio, the c_p based on shaft power was significantly reduced due to the drag losses. Based on the bare rotor disk area, the maximum increase in peak c_p was 55% and the tip speed ratio curves were again narrow and sharply peaked. The drag losses appeared to be partially due to stalled regions on the tip vanes and partially due to residual induced drag. Subsequent tests with linearly twisted tip vanes eliminated the partial tip vane stall but could not completely reduce the residual induced drag. Although the twisted tip vanes were less effective in increasing the peak power coefficient, the tip speed ratio curves were broadened with the emergence of a second peak on the curve at a higher tip speed ratio. A summary of the results obtained in the wind tunnel, tow, and water channel tests is contained in Table 4.

The water channel tests by AeroVironment, Inc., indicate that high shaft power augmentation approaching the demonstrated flow augmentation

Run No.	Tip Speed Ratio	Power Coefficient Based on Shaft Power		Power Coefficient Based on Wake Deficit	
		Theoretical	Experimental	Theoretical	Experimental
48	3	—	0.49	—	0.70
48	6	0.75	0.20	0.98	1.30
59	6	0.80	0.18	1.06	0.90

Table 3. Comparisons of Theoretical Predictions and Experimental Observations of Dynamic Inducer Performance for Two Test Runs in the Water Channel (Based on effective rotor area which includes tip vanes) (from Ref. 20).

Tests	Based on Bare Rotor Area	Based on Effective Area (includes tip vanes)
Wind Tunnel	70%	—
Tow (Field)	35%	—
Water Channel (Untwisted Tip Vanes)	55%	25%
Water Channel (Twisted Tip Vanes)	40%	15%

Table 4. Experimentally Observed Augmentation of Peak Power Coefficient by the Dynamic Inducer (Based on bare rotor performance).

may be feasible if tip vanes can be designed to significantly reduce the induced drag. This might be accomplished through more detailed theoretical analysis of the flow domain and, if warranted, experimental verification. Ideally this type of analysis would generate tip vane designs which both greatly enhance shaft power augmentation and provide broader power coefficient versus tip speed ratio curves.

5. VAWT AIRFOIL CONFIGURATIONS

Research on higher performance airfoils for vertical axis wind turbines (VAWT) has been in progress since 1977 under ERDA, DOE, and SERI support. Most of the early work at West Virginia University (WVU) was concentrated on circulation controlled airfoils (21). Two promising offshoots of the VAWT research at WVU are the investigation of higher performance airfoils for VAWT by Melior Corporation (22) and research on the elimination of adverse flow curvature effects on VAWT airfoils, begun at WVU (23) and continued by Melior Corporation (22).

The study of higher performance airfoils has investigated improving lift-drag characteristics by employing low drag airfoil shapes such as the NACA 63_b-0XX and NACA 64_b-0XX series (22). The NACA-00XX airfoils, the most commonly used airfoils for VAWT, provided a baseline for performance comparisons. The performance of each airfoil was derived from a blade element-momentum theory developed for VAWT, with lift and drag coefficients obtained from available literature on steady state airfoil data for a constant chord Reynolds number (Re) of $\sim 3.0 \times 10^6$. Because of the constant Re assumption, the predicted performance for each airfoil is probably too high, but the relative comparisons between airfoils are presumably valid.

The results of the analysis indicate that the low drag airfoils, led by the NACA 63_b-0XX series, would provide better performance characteristics. Comparisons of the NACA 63_2-015 with NACA 0015 are shown in Figures 14 and 15. Figure 14 shows power coefficient (c_p) as a function of tip speed ratio for these two airfoils at two different rotor solidities (σ). These results demonstrate the potential of the NACA 63_b-0XX airfoil series for significantly enhancing VAWT performance at the higher tip speed ratios. The potential increase in annual energy output (AEO) predicted for the NACA 63_2-015 airfoil is shown as a function of rotor solidity in Figure 15. Within the range of rotor solidity used in the analysis, the predicted AEO is 17-27%

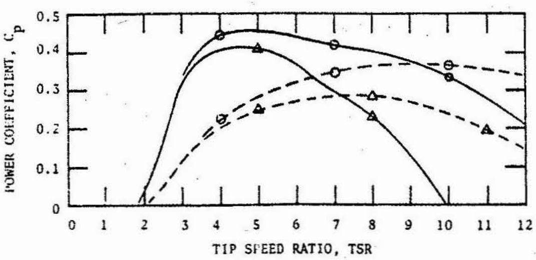

Fig. 14. Power Coefficient (c_p) vs. Tip Speed Ratio for the NACA 63_2-015 and NACA 0015 Airfoils (- - - σ=0.07, —— σ = 0.21, -NACA 63_2-015, △-NACA 0015) (from Ref. 22).

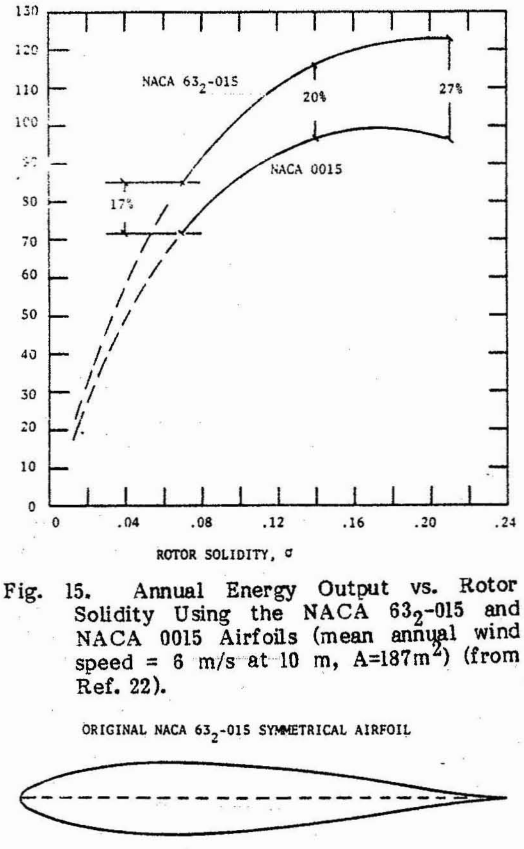

Fig. 15. Annual Energy Output vs. Rotor Solidity Using the NACA 63_2-015 and NACA 0015 Airfoils (mean annual wind speed = 6 m/s at 10 m, A=187m^2) (from Ref. 22).

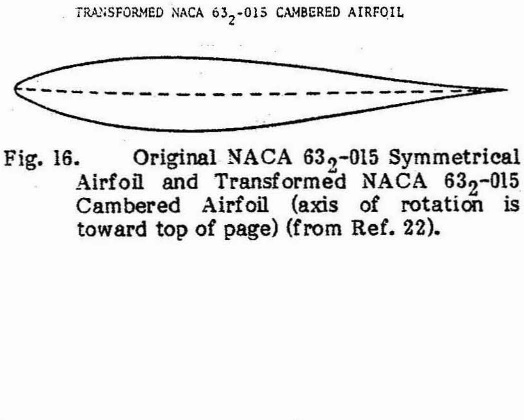

Fig. 16. Original NACA 63_2-015 Symmetrical Airfoil and Transformed NACA 63_2-015 Cambered Airfoil (axis of rotation is toward top of page) (from Ref. 22).

higher than that of the NACA 0015 airfoil.

Based on these results, low drag airfoils warrant further investigation for use in VAWT. Of primary importance is the actual potential for increased AEO relative to the commonly used NACA 00XX airfoil series. However, the relative dynamic response characteristics of each airfoil must also be considered. Potential aeroelastic and aeroacoustic levels will be dependent on the dynamic response of each airfoil to atmospheric turbulence, to the wake generated by the rotor support column, and to the wakes self generated by the airfoils during the upwind half of the rotation.

Research on VAWT aerodynamics has demonstrated, both analytically and experimentally, that VAWT turbine blades experience adverse flow curvature effects (23). These effects are due to the apparent (or effective) camber and incidence of a geometrically symmetric airfoil caused by the rotational path of the airfoil, boundary layer centrifugal effects, and the curvilinear flow field seen by the rotor. However, the aerodynamic characteristics of the airfoils used in VAWT are based on rectlinear flow. Analysis has indicated that a slightly cambered airfoil, obtained by conformally mapping a symmetrical airfoil (Figure 16), can eliminate adverse flow curvature effects. The performance of the cambered airfoil would then be nearly equivalent to that of the symmetric airfoil in rectilinear flow.

6. PASSIVE CYCLIC PITCH VARIATION

The Passive Cyclic Pitch concept incorporates a two-bladed HAWT teetered about an axis set at a pre-lag angle of 23° from the blade axis (Figure 17). This gives a large delta three angle (δ_3) of 67° as measured from the axis perpendicular to the blade axis. Teetering of the rotor eliminates gyroscopic moments during yaw. However, a conventional teeter hinge at 90° from the blade axis (δ_3=0) can produce periodic in-plane blade excursions if the blades have built-in or elastic coning and if nonzero yaw angles, yawing, or nonuniform inflow causes blade flapping about the teeter hinge (24). The resulting blade angular velocity variations cause dynamic loads leading to vibrations, fatigue, and teeter instability. Rotors with conventional delta three blade hinges ($\delta_3 \leq 30°$) are similarly affected. Use of the small pre-lag (or large δ_3) angle for the teeter hinge in the Passive Cyclic Pitch concept provides a strongly negative pitch-flap coupling which suppresses blade flapping and the associated dynamic loads. Thus an unbalancing gyroscopic or aerodynamic moment causes cyclic pitch variation which eliminates the imbalance. However, the steady state power output is unaffected by passive blade cyclic pitch variation.

The Passive Cyclic Pitch concept can provide several performance and cost benefits. Reducing dynamic loads on the rotor support and yaw instabilities due to negative yaw damping

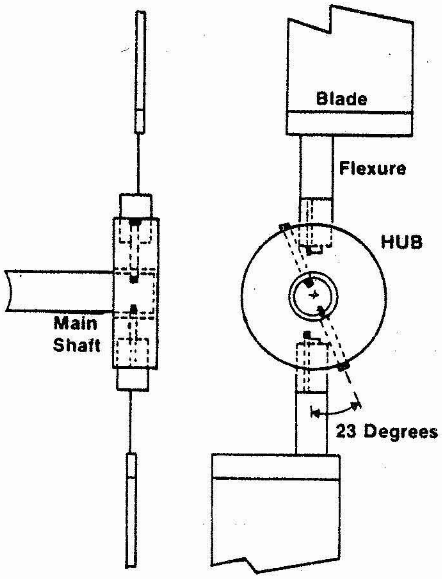

Fig. 17. Sketch of a Two-Bladed HAWT with Passive Cyclic Pitch.

while eliminating gyroscopic moments can lower structural requirements and costs for a HAWT. Because of the reduced dynamic loads at high yaw angles and yaw rates, the Passive Cyclic Pitch concept can employ less costly and more reliable rotor yaw or furling rather than blade feathering as a means of rotor torque and/or speed control. The elimination of gyroscopic moments also removes turbine size limitations on the use of tail vane stabilization (i.e., passive yaw control) for upwind HAWT.

For large wind turbines, the elimination of gyroscopic moments would permit higher yaw rates and, hence, increased energy capture. Preliminary estimates of the increase in annual energy output are in the neighborhood of 5%. For small wind turbines, the Passive Cyclic Pitch concept can facilitate reducing the blade number to two, thus reducing rotor costs. Small turbines generally have three or more blades as two-bladed turbines with rigid blade-hub attachments can experience severe two per rev (2P) vibrations.

6.1 Research on the Passive Cyclic Pitch Concept

The Passive Cyclic Pitch concept has been investigated by Washington University Technology Associates, Inc., and by Washington University under SERI support since 1979. Initial research involved wind tunnel testing of a 0.437m (1.43 ft) diameter model operating without power extraction. These tests verified the predicted operational characteristics of the concept (25). Detailed analytical models were then developed and applied to the design of a 7.62m (25 ft) diameter field test model, shown with the rotor completely furled in Figure 18. Atmospheric tests of this model demonstrated the technical

Fig. 18. Atmospheric Model with Passive Cyclic Pitch-Rotor is in Furled Position.

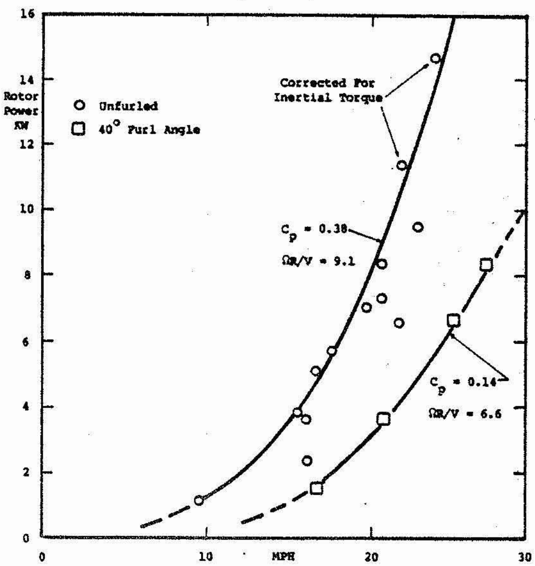

Fig. 19. Rotor Power vs. Wind Speed for Unfurled Rotor and for 40° Furl Angle (from Ref. 25).

viability of the Passive Cyclic Pitch concept (25). Measured rotor power versus wind speed for both the unfurled rotor and the 40° furl angle are shown in Figure 19. Figure 20 shows the predicted yaw response, based on the experimental results, of a MOD-OA size rotor with passive blade cyclic pitch variation compared to the actual design yaw response of

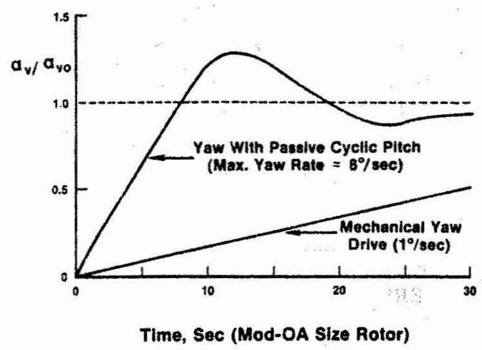

Fig. 20. Yaw Response to a Step Wind Direction Change of $\alpha_{VO}=60^{0}$ for V_{∞} = 9.5 m/s (from Ref. 25).

the MOD-OA for a step change in the wind direction of 60° in a 9.5 m/s wind.

Subsequent research efforts have been concentrated on adding an automatic yaw or furl control system (26). Atmospheric tests with the 7.26m (25 ft) diameter model indicated that a simple and reliable passive mechanical furling system could accurately control rotor speed and torque. These tests were conducted with both a variable speed alternator and a constant speed induction generator interconnected with a utility grid. A detailed dynamic yawing analysis was developed in conjunction with the field tests. Current research efforts at Washington University are investigating additional modifications, such as elastic restraint of the cyclic pitch motion, to further optimize the field test model.

6.1.1 Proof of Concept Testing

A 7.62m (25 ft) diameter prototype of the Passive Cyclic Pitch concept is presently undergoing Proof-of-Concept testing at the Rocky Flats Small Wind Systems Test Center. The prototype is similar in design to the 7.62m (25 ft) diameter field test model yet incorporates several modifications (e.g., shorter blade shanks) to improve rotor performance and operation. Initial results of the Proof-of-Concept tests should be forthcoming in the near future.

7. CONCLUSIONS

The five AIWEC discussed in the present paper are concepts in the AIWEC research program at SERI which have shown some promise of technical and economic viability. One of these concepts, Passive Cyclic Pitch Variation with automatic yaw or furl control, has reached a Proof-of-Concept phase of testing at the Rocky Flats Small Wind Systems Test Center. The other four, the Diffuser Augmented Wind Turbine (DAWT), the Electrofluid Dynamic (EFD) wind-driven generator, the Dynamic Inducer, and higher performance VAWT Airfoil Configurations are in various stages of research. Of the latter four, the DAWT has reached the most advanced stage of development. Additional R&D is needed to more definitively determine the potential of each of these concepts.

8. NOMENCLATURE

A	rotor cross-sectional area
AEO	annual energy output
$\bar{c}$	mean chord length
COE	annualized cost of energy
c_p	power coefficient ($=P/\frac{1}{2}\rho A V_{\infty}^3$)
NACA	National Advisory Committee for Aeronautics
P	power output
R	rotor radius
Re	Reynolds number
V_{∞}	ambient wind velocity
X	tip speed ratio ($=\Omega R/V$)
x_T	tip vane angle measured from perpendicular to blade axis
x_V	wind direction relative to turbine orientation
δ_3	blade hinge angle measured from perpendicular to blade axis
Ω	rotor angular velocity
ρ	ambient air density
σ	rotor solidity - ratio of total blade planform area to rotor cross-sectional area

REFERENCES

(1) Furuya, O. and Maekawa, S., "Technical and Economical Assessment on Tethered Wind Energy Systems (TWES), SERI/TR-09172-2, Tetra Tech, Inc., Pasadena, CA, June 1982.

(2) Minardi, J.E., Lawson, M.O., Williams, G., "Electrofluid Dynamic (EFD) Wind Driven Generator," NSF Report COO/4130-77/1, Oct. 1976, University of Dayton Research.

(3) Minardi, J.E., Lawson, M.O., "Annual Progress Report on the Electrofluid Dynamic Wind Driven Generator," ERDA Report COO/4130-77/2, July 1977, University of Dayton Research Institute, Dayton, Ohio.

(4) Minardi, J.E., Lawson, M.O., Wattendorf, F.L., "Third Annual Progress Report on the Electrofluid Dynamic Wind Generator," DOE Report COO-4130-2, May 1979, University of Dayton Research Institute, Dayton, Ohio.

(5) Minardi, J.E., Lawson, M.O., Wattendorf, E.L., "Fourth Annual Progress Report on the Electrofluid Dynamic Wind Generator," UDR-TR-80-108, May 1981, University of Dayton Research Institute, Dayton, Ohio.

(6) Minardi, J.E. and Lawson, M.O., "Conceptual Design of an Electrofluid Dynamic Wind Energy System," SERI/TR-1-1291-1, to be published by SERI, University of Dayton Research Institute, Dayton, OH.

(7) Mitchell, R.L., "Analysis of the Potential of the Electrofluid Dynamic Wind-Driven Generator," Solar Engineering 1983, Proceedings of the 5th Annual Technical Conference of the Solar Energy Division of ASME, Orlando, FL, April 19-21, 1983.

(8) "MOD-2 Wind Turbine System Concept and Preliminary Design Report," Volume II Detailed Report, DOE/NASA 0002-80/2, (also NASA CR-159609), July 1979, Boeing Engineering and Construction, Seattle, Wash.

(9) "Selected Climatic Maps of the United States," 1977, National Climatic Center, Ashville, NC.

(10) McConnell, R.D., "Giromill Overview," SERI/TP-35-263, May 1979, Solar Energy Research Institute, Golden, CO.

(11) McConnell, R.D., "A Screening Method for Wind Energy Conversion Systems," SERI/TP-731-649, June 1980, Solar Energy Research Institute, Golden, CO.

(12) Foreman, K.M., "Economics of DAWT Wind Energy Systems," SERI/CP-635-1340 (also CONF-811043), Proceedings of the Fifth Biennial Wind Energy Conference and Workshop (WWV), Washington, D.C., Oct. 5-7, 1981, pp. 469-485.

(13) Lilley, G.M. and Rainbird, W.J., "A Preliminary Report on the Design and Performance of Ducted Windmills," Report 102, April 1956, College of Aeronautics, Cranfield, England. (Also available as Technical Report C/T 119, 1957, Electrical Research Assoc., Leatherhead, England).

(14) Foreman, K.M. and Gilbert, B.L., "Further Investigations of Diffuser Augmented Wind Turbines, Part II—Technical Report," DOE Report COO-2616-2 (Part 2) (Rev. 2), July 1979, Grumman Aerospace Corp., Bethpage, NY.

(15) Oman, R.A., Foreman, K.M., and Gilbert, B.L., "Investigation of Diffuser Augmented Wind Turbines, Part II—Technical Report," ERDA Report COO-2616-2 (also available as Grumman Research Dept. Report RE-534), January 1977, Grumman Aerospace Corp., Bethpage, NY).

(16) Foreman, K.M., "Preliminary Design and Economic Investigations of Diffuser Augmented Wind Turbines (DAWT)," SERI/TR-98073-18, December 1981, Grumman Aerospace Corp., Bethpage, NY.

(17) Foreman, K.M., Maciulaitis, A., and Gilbert, B.L., "Performance Predictions and Recent Data for Advanced DAWT Models," Solar Engineering - 1983, Proceedings of the ASME Solar Energy Division Fifth Annual Conference, Orlando, FL, April 18-21, 1983, pp. 596-605.

(18) Lissaman, P.B.S. and Walker, S., "Dynamic Inducer Research Program," DOE Report RLO-1021-77/1, June 1978, AeroVironment Inc., Pasadena, CA.

(19) Lissaman, P.B.S., Zalay, A.D., and Hibbs, B.H., "Advanced and Innovative Wind Energy Concept Development: Dynamic Inducer System," SERI/TR-9-8085-1b, August 1981, AeroVironment, Inc., Pasadena, CA.

(20) Gyatt, G.W., Zalay, A.D, and Hibbs, B., "Optimization of the Dynamic Inducer Wind Energy Systems," SERI/TR-1-1167-1, to be published by SERI, AeroVironment, Inc., Pasadena, CA.

(21) Walters, R., Wolfe, W.P., and Migliore, P.G., "Vertical Axis Wind Turbine Research at West Virginia University," SERI Second Wind Energy Innovative Systems Conference, SERI/CP-635-938, Colorado Springs, CO, December 3-5, 1980, pp. 159-178.

(22) Migliore, P.G. and Fritschen, J.R., "Darrieus Wind Turbine Airfoil Configurations," SERI/TR-11045-1, June 1982, Melior Corp., Davis, CA.

(23) Migliore, P.G. and Wolfe, W.P., "The Effects of Flow Curvature on the Aerodynamics of Darrieus Wind Turbines," DOE Report ORO/5135-77/7, July 1980, West Virginia University, Morgantown, WV.

(24) Hohenemser, K.H. and Swift, A.H.P., "On the Design of Horizontal Axis Two-Bladed Hinged Wind Turbines," Solar Engineering - 1983, Proceedings of the ASME Solar Energy Division Fifth Annual Conference, Orlando, FL, April 18-21, 1983, pp. 583-589.

(25) Hohenemser, K.H., Swift, A.H.P., and Peters, D.A., "The Yawing of Wind Turbines with Blade Cyclic Pitch Variation," SERI/TR-9-8083-3a, August 1981, Washington University Technology Associates, Inc., St. Louis, MO.

(26) Hohenemser, K.H. and Swift, A.H.P., "The Investigation of Passive Blade Cyclic Pitch Variation Using an Automatic Yaw Control System," SERI/TR-11052-2, August 1982, Washington University Technology Associates, Inc., St. Louis, MO.